Activation Energies and Beyond

Zeke A. Piskulich,[1] Oluwaseun O. Mesele,[1] and Ward H. Thompson[1, a)]
Department of Chemistry, University of Kansas, Lawrence, KS 66045, USA

Recent advances in the calculation and interpretation of the activation energy for a dynamical process are described. Specifically, new approaches that apply the fluctuation theory of statistical mechanics to dynamics enable the direct determination of the activation energy for an arbitrary dynamical timescale from simulations at a single temperature. This opens up significant new possibilities for understanding activated processes in cases where a traditional Arrhenius analysis is not possible. The methods also enable a rigorous decomposition of the activation energy into contributions associated with the different interactions and motions present in the system. These components can be understood in the context of Tolman's interpretation of the activation energy. Specifically, they provide insight into how energy can be most effectively deposited to accelerate the dynamics of interest, promising important new mechanistic information for a broad range of chemical processes. The general approach can be extended beyond activation energies to the examination of non-Arrhenius behavior as well as the changes in dynamical timescales with respect to other thermodynamic variables such as pressure.

I. INTRODUCTION

The activation energy for a thermal reaction rate constant, $k(T)$, defined as

$$E_a = -\frac{\partial \ln k(T)}{\partial \beta}, \tag{1}$$

where $\beta = 1/k_B T$, is one of the most fundamental characteristics of the underlying chemical process. It is most often interpreted in relation to the Arrhenius expression for the rate constant,[1–4]

$$k(T) = A\, e^{-E_a/k_B T}, \tag{2}$$

where A is the Arrhenius prefactor, or frequency factor, that is assumed to be temperature independent. This empirical relationship between the rate constant and temperature gives rise to the standard approach for determining the activation energy: one constructs an Arrhenius plot of $\ln k(T)$ versus $1/T$ and the slope is then $-E_a/k_B$. The resulting E_a is frequently related to the barrier for the reaction, which can be valuable for gaining insight into the reaction mechanism.

There are important limitations to obtaining the activation energy by an Arrhenius analysis. The requirement that k be measured or calculated over a range of temperatures cannot be met in some cases. For example, near a phase transition an increase or decrease in temperature can lead to a change in k that is due to the phase change rather than the barrier in the state of interest. Proteins and other biomolecules that undergo folding/unfolding transitions represent a special case of this problem in which only a limited temperature range is available for an Arrhenius analysis. This constraint competes with the requirement that the temperature range must also be sufficiently broad that changes in k are large enough to be resolved by the experimental or simulation approach.

Activation energies are relevant for many timescales other than chemical reaction rate constants and the conflicts inherent in choosing an appropriate temperature range can be particularly prominent in such cases. Diffusion coefficients, reorientation times, viscosity, and dielectric relaxation times are only a few examples of timescales that can be described by an Arrhenius equation analogous to Eq. 2. Because the underlying processes do not involve changes in chemical bonding, they typically have smaller activation energies and thus depend more weakly on temperature. Moreover, the interpretation of the activation energy is more challenging in such cases, for which a clear reaction coordinate and barrier are not readily identifiable.

In this Article, we discuss recently developed approaches for avoiding an Arrhenius analysis by direct calculation of the activation energy from simulations at a single temperature. In general terms, these methods focus on calculation of the analytical derivative of an arbitrary dynamical timescale with respect to temperature, in contrast to the numerical derivative obtained in an Arrhenius analysis. Conceptually, the approach is essentially the fluctuation theory of statistical mechanics applied to dynamics. As such, it permits not only comptutational advantages, but new physical insight that is otherwise inaccessible.

Nearly a century ago, Tolman developed, based on a statistical mechanical analysis, an alternative interpretation of the activation energy as the difference in the average energy of reacting molecules minus the average energy of reactant molecules,[5]

$$E_a = \langle E \rangle_{reacting} - \langle E \rangle_r, \tag{3}$$

This idea was further developed by Truhlar[6] in terms of the reactive cross sections of gas phase collision theory which improved upon an approximation in Tolman's approach. Note that the focus of Tolman's interpretation is on the energy the reacting species must have to overcome the barrier rather than the height of the barrier that must be overcome. This is a different perspective than is often used in thinking about activation energies and it opens up

a)Electronic mail: wthompson@ku.edu

new possibilities for physical insight.[7–9] In particular, it indicates that the activation energy can be decomposed into contributions due to the system interactions (*vide infra*). A given component is then the average energy of the reacting species, relative to that of the reactants, associated with the specific interaction. The contribution to the activation energy is then the measure of how effective additional energy in this interaction is for speeding up the dynamics of interest.

The remainder of this Article is organized as follows. We first introduce the Tolman interpretation of activation energy and the fluctuation theory for dynamics approach using simple derivations; the implications for obtaining new mechanistic insight using this method are discussed. Several examples of applications of this fluctuation theory are presented to illustrate the generality and flexibility of the method. Prospects for moving beyond the calculation of activation energies is then examined in terms of both non-Arrhenius behavior and derivatives of dynamical timescales with respect to other thermodynamic variables. We conclude with a brief summary and some remarks about future directions.

II. ACTIVATION ENERGIES

A. Interpretation

The Tolman interpretation of the activation energy, discussed above and expressed in Eq. 3, is most easily summarized by considering the thermal reaction rate constant written in terms of the cumulative reaction probability, $N(E)$; see, *e.g.*, Ref. 7. In brief, quantum mechanically $N(E)$ is the sum over all state-to-state reaction probabilities at a fixed total energy,[10]

$$N(E) = \sum_{\mathbf{n}_r,\mathbf{n}_p} P_{\mathbf{n}_r,\mathbf{n}_p}(E), \tag{4}$$

where $\mathbf{n}_r$ and $\mathbf{n}_p$ represent the full set of reactant and product quantum numbers. The classical $N(E)$ can be analogously defined. The reaction rate constant is given by

$$k(T) = \frac{1}{2\pi\hbar Q_r(T)} \int_0^\infty N(E)\, e^{-\beta E}\, dE, \tag{5}$$

where $Q_r(T)$ is the reactant partition function. Then it is straightforward to see that the activation energy is

$$E_a = \frac{\int_0^\infty N(E)\, E\, e^{-\beta E}\, dE}{\int_0^\infty N(E)\, e^{-\beta E}\, dE} + \frac{1}{Q_r}\frac{\partial Q_r}{\partial \beta}. \tag{6}$$

The second term can easily be identified as the negative of the average reactant energy, $-\langle E\rangle_r$. If we recognize

$$P_{reacting}(E) = \frac{N(E)\, e^{-\beta E}}{\int_0^\infty N(E)\, e^{-\beta E}\, dE}, \tag{7}$$

as the normalized distribution for the probability of reacting with a total energy E, then we can see that the first term in Eq. 6 is the average energy of species that react:

$$\langle E\rangle_{reacting} = \int_0^\infty E\, P_{reacting}(E)\, dE, \tag{8}$$

such that the activation energy is given by Eq. 3, as originally obtained by Tolman.[5]

It is useful to compare this to the activation energy one obtains from transition state theory[11,12] (TST) in which the rate constant is approximated as

$$k_{TST}(T) = \frac{k_B T}{h}\frac{Q^\ddagger}{Q_r}\, e^{-\beta E^\ddagger}, \tag{9}$$

where $Q^\ddagger$ and $E^\ddagger$ are the transition state internal partition function and electronic energy, respectively. The activation energy is then given as

$$E_a^{TST} = E^\ddagger + \langle E\rangle_{int,\ddagger} + k_B T - \langle E\rangle_r, \tag{10}$$

where $\langle E\rangle_{int,\ddagger} = -\partial \ln Q^\ddagger/\partial\beta$ is the average internal (rotational and vibrational) energy of the transition state structure or "activated complex." Comparing this result with Eq. 3 indicates that within TST the average energy of reacting species is $\langle E\rangle^{TST}_{reacting} = E^\ddagger + \langle E\rangle_{int,\ddagger} + k_B T$. That is, $\langle E\rangle^{TST}_{reacting}$ is the electronic barrier height plus the average thermal internal energy of the transition state and $k_B T$ associated with kinetic energy along the reaction coordinate.

If we note that the exact rate constant can be written as

$$k(T) = \kappa(T)\, k_{TST}(T), \tag{11}$$

where $\kappa(T)$ is the transmission coefficient, then it is straightforward to see that

$$E_a = E_a^{TST} + E_{a,\kappa}. \tag{12}$$

Here, $E_{a,\kappa} = -\partial \ln\kappa/\partial\beta$ is the contribution to the activation energy from the temperature dependence of the transmission coefficient. Since $\kappa(T)$ corrects all sins of the TST approximation, it can include, for example, contributions from both transition state recrossing and quantum mechanical tunneling. Moreover, it is important to note that, like k_{TST}, $\kappa(T)$ depends on the choice of the transition state dividing surface that separates the reactants and products. This is evident from Eq. 11 because the exact (measurable) rate constant, $k(T)$, does not depend on any definition of a transition state while $k_{TST}(T)$ naturally does. Consequently, both E_a^{TST} and $E_{a,\kappa}$ are not obtainable from measurements because they depend on the choice of the dividing surface separating reactants and products, while E_a does not.

The above results lead to some of the commonly invoked intepretations of the activation energy that differ from that of Tolman and must be applied with care. For

example, the activation energy is often loosely considered to represent the barrier height for the reaction. This is a reasonable extension of Eq. 3 since the energy of reacting species above that of reactants is related to the barrier height that must be surmounted to react. However, this equivalence should not be taken too literally; for example, as we show below, the average energy of the reacting species, $\langle E\rangle_{reacting}$, and the reactants, $\langle E\rangle_r$, can be decomposed into various energy components and thus so can the activation energy, in a way that does not make sense for the barrier height. That is, the activation energy is a measure of the *energy required to surmount the barrier* and not just the electronic (or even thermal) energy of the barrier.

B. Fluctuation Theory for Dynamics

1. Derivation

Fluctuation theory has been used to great effect in understanding equilibrium statistical thermodynamics,[13–15] but only recently has it been shown that the same ideas can be extended to understand chemical dynamics. A prototypical example of fluctuation theory is the relation between the heat capacity and energy fluctuations. Namely, the average energy of a system in the canonical ensemble is given by

$$\langle E\rangle = -\frac{\partial \ln Q(N,V,T)}{\partial \beta}, \tag{13}$$

where Q is the partition function. Then, the heat capacity, C_V, is obtained by taking the temperature derivative of $\langle E\rangle$ and can be shown to be related to the fluctuations in the energy,[13]

$$C_V = \left(\frac{\partial\langle E\rangle}{\partial T}\right)_{N,V} = \frac{1}{k_B T^2}\left[\langle E^2\rangle - \langle E\rangle^2\right] = \frac{\langle \delta E^2\rangle}{k_B T}, \tag{14}$$

where $\delta E = E - \langle E\rangle$ is the fluctuation of the system energy from its equilibrium average.

This framework for connecting thermodynamic properties, particularly those that are related to derivatives of averages with respect to thermodynamic variables, can be straightforwardly generalized to dynamical properties. To see this, consider some property $f(t) = f(\mathbf{p},\mathbf{q},t)$ that depends on the system momenta ($\mathbf{p}$) and coordinates ($\mathbf{q}$). Here, we assume a classical system, though a quantum mechanical version of the following result is obtainable in a completely analogous way. The average of the property f in the canonical ensemble can then be written as

$$\begin{aligned}\langle f(t)\rangle &= \frac{1}{Qh^F}\int\int d\mathbf{p}\, d\mathbf{q}\, e^{-\beta H(\mathbf{p},\mathbf{q})}\, f(\mathbf{p},\mathbf{q},t),\\ &= \frac{1}{Q}\mathrm{Tr}[e^{-\beta H}\, f(t)],\end{aligned} \tag{15}$$

where F is the number of degrees-of-freedom, Q is the canonical partition function, and the second equality defines the trace, Tr, as an average over phase space. Then, because only Q and the Boltzmann weight depend on temperature (note the similarity to Eq. 5),

$$\begin{aligned}\frac{\partial\langle f(t)\rangle}{\partial\beta} &= -\frac{1}{Q}\frac{\partial Q}{\partial\beta}\langle f(t)\rangle - \frac{1}{Q}\mathrm{Tr}[e^{-\beta H}\, H(0)\, f(t)]\\ &= -\frac{1}{Q}\mathrm{Tr}[e^{-\beta H}\,\delta H(0)\, f(t)]\\ &= -\langle \delta H(0)\, f(t)\rangle,\end{aligned} \tag{16}$$

where $\delta H(0) = H(0) - \langle H\rangle$. This result has a simple physical interpretation as discussed in the following section and illustrated in Fig. 1. We can also note that if $f(t) = \delta H(0) = \delta E(0)$ then this result is the same as Eq. 14 for the heat capacity.

If $f(t)$ is chosen to be a dynamical variable, the resulting derivative in Eq. 16 gives the temperature dependence of the corresponding transport coefficient or dynamical timescale. In one general case, $f(t)$ can represent a time-correlation function (TCF), $C(t) = \langle A(0)\, B(t)\rangle$, where A and B are two functions of phase space coordinates. Typically, a dynamical constant of interest can be obtained from the time decay or integral of the TCF; several examples are given below. The result in Eq. 16 gives the temperature (or, equivalently, β) derivative of the entire TCF as $\frac{\partial C(t)}{\partial\beta} = -\langle \delta H(0)\, A(0)\, B(t)\rangle$. In this regard, the fluctuation theory applied to dynamics is quite powerful as it provides more than just an activation energy for a single timescale.

2. Mechanistic Insight

One of the advantages of this fluctuation theory approach is that it can provide physical insight that is not readily available from other methods. For example, the temperature (β) derivative of the average time-dependent property in Eq. 16 involves fluctuations in the full, system energy, $\delta H(0)$. The interpretation of this, illustrated in Fig. 1, is straightforward: the derivative is a measure of how the dynamics characterized by $\langle f(t)\rangle$ are accelerated or retarded when there is more ($\delta H > 0$) or less ($\delta H < 0$) energy available than average.

The total system energy can also be decomposed into additive components in an almost endless number of ways to provide mechanistic insight. That is, if $H = \sum_\alpha H_\alpha$, then

$$\frac{\partial\langle f(t)\rangle}{\partial\beta} = -\sum_\alpha \langle \delta H_\alpha(0)\, f(t)\rangle. \tag{17}$$

Then each term has the interpretation of the contribution of the H_α energy to the change in $\langle f(t)\rangle$ with β. Namely, it is a measure of how the dynamics of $\langle f(t)\rangle$ are modified when there is more ($\delta H_\alpha > 0$) or less ($\delta H_\alpha < 0$) of the H_α energy component available relative its average value.[16]

In the simplest case, one can write the total Hamiltonian in many classical simulations as $H = KE +$

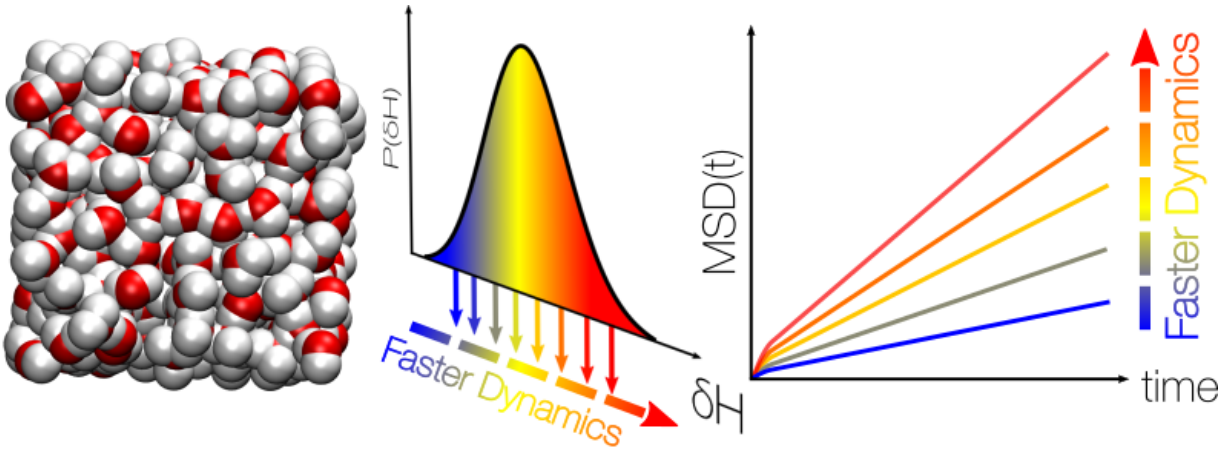

FIG. 1: Schematic illustration of the fluctuation theory for dynamics. An MD simulation in the canonical ensemble (left) exhibits a distribution of total energies with fluctuations, δH, about the average value (center). Higher energies lead to faster dynamics, such as diffusion (right), while smaller energies lead so slower dynamics. The change in the dynamical timescale, *e.g.*, diffusion coefficient, with the energy is measured by the activation energy.

$V_{LJ} + V_{Coul} + V_{intra}$, where KE, V_{LJ}, V_{Coul}, and V_{intra} are the kinetic energy and Lennard-Jones, Coulombic, and intramolecular potential energy terms, respectively. Then, for example, $-\langle \delta V_{Coul}(0)\, f(t)\rangle$ is the contribution to the β derivative of $\langle f(t)\rangle$ that is associated with the Coulombic interactions. If $\langle f(t)\rangle$ is related to a dynamical timescale (*e.g.*, rate constant, reorientation time), this provides a way to determine the contributions of the different energetic terms in the system to the activation energy associated with the timescale. In the context of Tolman's interpretation of the activation energy given in Eq. 3, this means one can determine, for example, $E_{a,Coul} = \langle E\rangle_{reacting,Coul} - \langle E\rangle_{r,Coul}$, which is the average *Coulombic* energy of reacting molecules minus the average *Coulombic* energy of reactant molecules. Because there are a multitude of ways to additively divide the contributions to the total Hamiltonian, the mechanistic information that can be obtained by this approach is considerable.

3. Other Ensembles

Fluctuation theory can also be applied in ensembles beyond the canonical one. For example, the activation energy for a dynamical process occurring at constant pressure, *i.e.*, in the isothermal-isobaric or NPT ensemble, can be obtained as well. In this case, the average of a dynamical property, f, is given by

$$\langle f(t)\rangle_p = \frac{1}{\Delta}\mathrm{Tr}[e^{-\beta(H+pV)}\, f(t)], \tag{18}$$

where $\Delta(N,p,T)$ is the isotherm-isobaric ensemble partition function. Then, it is straightforward to show that the derivative of the average $f(t)$ at constant pressure is

$$\begin{aligned}\frac{\partial\langle f(t)\rangle_p}{\partial\beta} &= -\frac{1}{\Delta}\mathrm{Tr}[e^{-\beta(H+pV)}\,(\delta H(0) + p\delta V(0))\, f(t)],\\ &= -\langle \delta H(0)\, f(t)\rangle_p - p\langle \delta V(0)\, f(t)\rangle_p. \end{aligned}\tag{19}$$

As will be shown below, the second term is related to the activation volume for the process while the first term is analogous to Eq. 16 but evaluated at constant pressure instead of constant volume. The difference between the constant volume and constant pressure activation energy has not received a great deal of attention, but both have been measured in some key cases, *e.g.*, for the diffusion coefficient of water.[17–20]

C. Examples

To illustrate the potential of this fluctuation theory for dynamics and detail the implementation, we consider some specific examples. In particular, we discuss the theoretical framework for many different dynamical timescales that are frequently of interest and present results for particular applications to three properties of one system, liquid water.

We have implemented Eq. 16 in multiple ways, the key feature of which is that the averages must be evaluated in in an ensemble with constant T where fluctuations in the system energy, δH, are present. In principle, this means that a single MD simulation where the temperature is maintained with a thermostat can be used to evaluate activation energies. While this can be straightforwardly implemented,[21] it is approximate because the thermostat affects the dynamics. In many cases, this approach can be sufficient to determine a reasonable activation energy. However, this issue can be avoided entirely by running a thermostatted trajectory at a temperature T to generate

initial conditions for subsequent short, constant energy, NVE, trajectories from which the dynamics and activation energies are obtained. Each short trajectory has its own fixed energy and hence fluctuation from the average of all the trajectories, δH. This approach has no effect from the thermostat (as long as it provides the correct distribution of energies) and has the advantage that the short trajectories are independent and can be run in an embarrassingly parallel fashion. Except where otherwise noted, the data presented here were obtained using this approach.

1. Reaction Rate Constant

A common approach to calculating the rate constant for a chemical reaction is through reactive flux TCFs,[22–24] such as

$$k(T) = \lim_{t \to long} \langle F_s(0)\, \mathcal{P}(t) \rangle. \tag{20}$$

Here, $F_s = \delta[s(0) - s^\ddagger]\, v_s(0)$ is the flux through the transition state dividing surface defined in terms of the reaction coordinate s with velocity v_s. The δ-function dictates that trajectories start at time $t = 0$ at the transition state defined by $s = s^\ddagger$ and $\mathcal{P}(t)$ is the characteristic function that is equal to 1 for reactive trajectories, *i.e.*, those that start as reactants in the past $(-t)$ and end as products in the future (t), and 0 for non-reactive trajectories. For example, $\mathcal{P}(t) = \Theta[s(t) - s^\ddagger]$, where $\Theta(x)$ is the Heaviside step function, is a common choice for evaluating the characteristic function. The exact classical rate constant is obtained when the trajectories are propagated to a time t long enough that all transition state recrossing has been completed.

The activation energy for the rate constant, Eq. 1, is then obtained using Eq. 16 as

$$E_a = \frac{\lim\limits_{t \to long} \langle \delta H(0)\, F_s(0)\, \mathcal{P}(t) \rangle}{\lim\limits_{t' \to long} \langle F_s(0)\, \mathcal{P}(t') \rangle}. \tag{21}$$

Such a result was first shown by Dellago and Bolhuis,[25] and has been implemented *via* transition path sampling simulations in a several cases.[26–31]

Interestingly, if this result is compared with the Tolman expression for the activation energy, Eq. 3, while noting that in this case of a chemical reaction $\delta H = H - \langle E \rangle_r$, it leads to the result

$$\langle E \rangle_{reacting} = \frac{\lim\limits_{t \to long} \langle H(0)\, F_s(0)\, \mathcal{P}(t) \rangle}{\lim\limits_{t' \to long} \langle F_s(0)\, \mathcal{P}(t') \rangle}, \tag{22}$$

for the average energy of the reacting species, which is equivalent to Eq. 8.

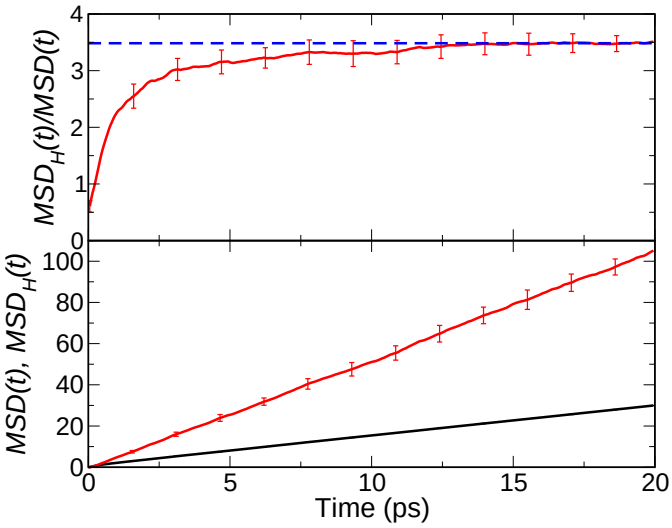

FIG. 2: Bottom: The TCFs $MSD(t)$ (black line) and $MSD_H(t)$ (red line) are plotted versus time for the SPC/E water model at 298 K obtained from 2,500 NVE trajectories. Top: The ratio $MSD_H(t)/MSD(t)$ (red line) is plotted as a function of time. A fit of this ratio between $t = 15 - 20$ ps to a constant value is also shown (blue dashed line). Note: $MSD(t)$ is in units of Å^2/ps, $MSD_H(t)$ in kcal/mol × Å^2/ps. Reprinted from Piskulich, Z. A., Mesele, O. O., and Thompson, W. H. *J. Chem. Phys.*, **2017**, *147*, 134103, with the permission of AIP Publishing.

2. Diffusion Coefficient

The diffusion coefficient, D, is typically calculated from the mean-squared displacement, $MSD(t) = \langle |\vec{r}(t) - \vec{r}(0)|^2 \rangle$, which is a measure of the distance traveled by a molecules in time t. Specifically, the diffusion coefficient is obtained as

$$D(T) = \lim_{t \to \infty} \frac{MSD(t)}{6t}, \tag{23}$$

for motion in three dimensions. Thus, in this case $f(t) = |\vec{r}(t) - \vec{r}(0)|^2$ and Eq. 16 leads to

$$\begin{aligned} E_{a,D} = -\frac{\partial \ln D}{\partial \beta} &= \frac{\lim\limits_{t \to \infty} \langle \delta H(0)\, |\vec{r}(t) - \vec{r}(0)|^2 \rangle}{\lim\limits_{t \to \infty} \langle |\vec{r}(t) - \vec{r}(0)|^2 \rangle} \\ &= \frac{\lim\limits_{t \to \infty} MSD_H(t)}{\lim\limits_{t \to \infty} MSD(t)}, \end{aligned} \tag{24}$$

where $MSD_H(t)$, defined by the last equality, is the mean-squared displacement weighted by the energy fluctuations.

In practice, Eq. 24 is most accurately evaluated by separately fitting $MSD_H(t)$ and $MSD(t)$ each to a line at longer times and then taking the value of the ratio of the slopes. In many cases, however, the activation energy

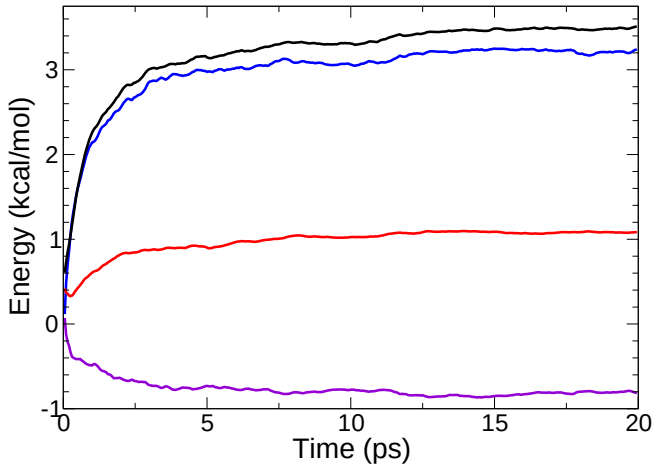

FIG. 3: The contributions to the diffusion TCF $MSD_H(t)$ shown in Fig. 2 associated with the kinetic energy (red line), Lennard-Jones potential energy (violet line), and Coulombic potential energy (blue line) are plotted versus time along with the total (black line). Reprinted from Piskulich, Z. A., Mesele, O. O., and Thompson, W. H. *J. Chem. Phys.*, **2017**, *147*, 134103, with the permission of AIP Publishing.

can be obtained from the ratio of the correlation functions directly at long times. This is illustrated in Fig. 2 where the mean-squared displacements (weighted and unweighted) and their ratio are shown for the SPC/E water model[32] at 298.15 K. From the data presented in Fig. 2, the activation energy for water diffusion is found to be $E_{a,D} = 3.48 \pm 0.16$ kcal/mol, in excellent agreement with $E_{a,D} = 3.49 \pm 0.20$ kcal/mol derived from an Arrhenius analysis.

As mentioned in the above section the fluctuation theory for dynamics offers new opportunities for insights into the mechanisms of diffusion by allowing for a decomposition of activation energies into various energetic contributions. In Fig. 3 we present the decomposition of the activation energy for the kinetic, Lennard-Jones, and electrostatic energy components with values of 1.1, -0.8, and 3.2 kcal/mol, respectively. This indicates that electrostatic interactions are the dominant contribution to the diffusion activation energy.

These results are indicative of the central role of hydrogen-bond (H-bond) exchanges in water diffusion, which are primarily governed by the electrostatic interactions. In the context of the Tolman interpretation of activation energies, this indicates that higher Coulombic interaction energy accelerates water diffusion, presumably by destabilizing the water H-bonds. In contrast, increasing the Lennard-Jones energy leads to *slower* diffusion; the reason for this is not yet completely clear, but is perhaps due to "jamming" of the water motion when the Lennard-Jones interactions are more repulsive. Furthermore, keeping in mind the Tolman interpretation of activation energies, this indicates that the water molecules with higher kinetic or electrostatic energies will diffuse more quickly on average than those that have larger Lennard-Jones energies.

3. Reorientational Timescales

Reorientational dynamics, as measured by infrared pump-probe anisotropy and spin-echo NMR, are characterized by the reorientation time correlation function, $C_2(t) = \langle P_2[\vec{e}(0) \cdot \vec{e}(t)]\rangle$. This TCF acts as a measure of the change in the orientation of a particular molecular axis, described by the unit vector $\vec{e}$, in time t. Here, P_2 denotes the second Legendre polynomial which weights the dynamics in accord with the IR spectroscopy and NMR signals. In this case then, $f(t) = P_2[\vec{e}(0) \cdot \vec{e}(t)]$ and thus from Eq. 16 we find that,

$$\frac{\partial C_2(t)}{\partial \beta} = -C_{2,H}(t) = -\left\langle \delta H(0) P_2\left[\vec{e}(t) \cdot \vec{e}(0)\right]\right\rangle . \quad (25)$$

For water reorientational dynamics we choose $\vec{e}$ to be along each OH bond. The OH reorientation dynamics exhibit three timescales: *1)* an inertial one ($\lesssim$25 fs) associated with water reorienting before it feels any other interactions, *2)* a librational one ($\lesssim$0.5 ps) associated with water rotations within a particular H-bond, and *3)* one associated with H-bond exchange dynamics ($\sim$3 ps). It is the last of these which is accessible to IR pump-probe anisotropy measurements.

These timescales can be extracted from the C_2 correlation function by fitting to a tri-exponential function,

$$C_2(t) = \sum_\alpha A_\alpha e^{-t/\tau_\alpha} = \sum_\alpha A_\alpha e^{-k_\alpha t}, \quad (26)$$

where α = inertial, librational, or 2 (associated with H-bond rearrangements) and A_α represents the amplitude (or importance) of the α reorientation timescale, $\tau_\alpha = 1/k_\alpha$. The reorientational TCF, from simulations using the TIP4P/2005 water model,[33] are shown in Fig. 4a along with the fit which yields $\tau_{iner} = 13$ fs, $\tau_{lib} = 0.455$ ps, and $\tau_2 = 3.2$ ps. NMR spin-echo experiments cannot access the individual timescales but instead measure the average reorientation time,[34]

$$\langle \tau_2 \rangle = \int_0^\infty C_2(t) dt. \quad (27)$$

For water, the integrated reorientation time is 2.2 ps for the TIP4P/2005 water model. Figure 4b shows both $C_2(t)$ and its time integral used to calculate this value.

The activation energies and temperature dependence of the amplitudes can be obtained by fitting the derivative TCF, $C_{2,H}(t)$, to the derivative of Eq. 26,

$$\frac{\partial C_2(t)}{\partial \beta} = \sum_\alpha \left[\frac{\partial A_\alpha}{\partial \beta} - A_\alpha \frac{\partial k_\alpha}{\partial \beta} t\right] e^{-k_\alpha t}. \quad (28)$$

using the amplitudes and timescales obtained from fitting $C_2(t)$ itself. Both the derivative TCF, $C_{2,H}(t)$, and its

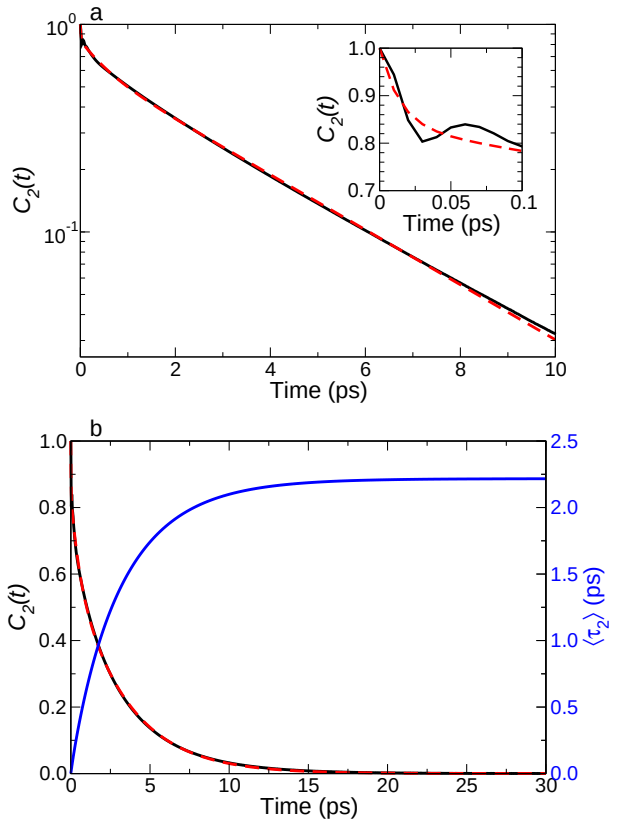

FIG. 4: OH reorientational correlation function, $C_2(t)$, (black) is shown as a function of time along with a triexponential fit (red), Eq. (26). a: $C_2(t)$ is shown on a semi-log scale and the short-time decay is shown in the inset. b: $C_2(t)$ is shown on a linear scale along with its integral (blue, right axis) which equals the average reorientational time, $\langle\tau_2\rangle$, at long times. Results are from 50,000 NVE trajectories with the TIP4P/2005 water model at 298.15 K and 1 bar. Reprinted from Piskulich, Z. A. and Thompson, W. H. *J. Chem. Phys.*, **2018**, *149*, 164504, with the permission of AIP Publishing.

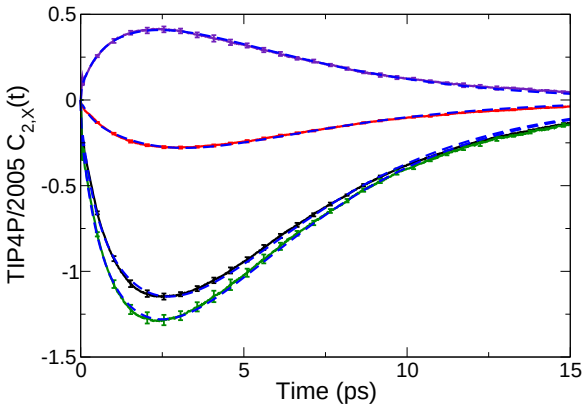

FIG. 5: The weighted reorientation correlation function $C_{2,H}(t)$ (black) corresponding to Fig. 4 is shown along with its contributions from the Lennard-Jones potential energy (indigo), electrostatic potential energy (green), and kinetic energy (red). Fits for each correlation function are included as blue dashed lines. Reprinted from Piskulich, Z. A. and Thompson, W. H. *J. Chem. Phys.*, **2018**, *149*, 164504, with the permission of AIP Publishing.

fit using this equation are shown in Fig. 5. From this, the activation energy of each reorientation timescale is calculated as,

$$E_{a,\tau_\alpha} = -\frac{1}{k_\alpha}\frac{\partial k_\alpha}{\partial \beta}, \tag{29}$$

Note that the activation energies for τ_{iner} and τ_{lib} are merely effective ones that describe the temperature dependence locally, as these timescales do not exhibit Arrhenius behavior.

The activation energy corresponding to the average reorientation time, $\langle\tau_2\rangle$, accessed by NMR is given by

$$E_{a,\langle\tau_2\rangle} = \frac{1}{\langle\tau_2\rangle}\int_0^\infty \frac{\partial C_2(t)}{\partial \beta}. \tag{30}$$

We have previously shown[35] that there is a quantitative and qualitative difference between the pump-prove activation energy, $E_{a,\tau_2} = 4.28\pm0.10$ kcal/mol, and the NMR activation energy, $E_{a,\langle\tau_2\rangle} = 4.58 \pm 0.11$ kcal/mol. This difference is associated with the change in the amplitude, A_2, which enters into the $\langle\tau_2\rangle$ activation energy.

As in the case of diffusion, the activation energies associated with OH reorientation in water can be decomposed into specific contributions from various components of the total energy. An example is shown in Fig. 5, where the weighted correlation functions for the kinetic, Lennard-Jones, and electrostatic energies are presented, corresponding to activation energy contributions of 1.14, -1.31, and 4.38 kcal/mol, respectively. As with diffusion, it is clear that the most important contribution to the activation energy comes from Coulombic interactions. Indeed, the results of this decomposition are in close accord with those from diffusion, reflecting the fact that H-bond exchanges are the key event in both the rotational and translational dynamics of water.

4. *Transport Coefficients*

Many important physical quantities may be calculated from the class of time correlation functions obtained as Green-Kubo relations. In a general context, a particular frequency-dependent transport coefficient can be expressed as a Fourier transform of the appropriate TCF,[36]

$$\sigma(\omega) = \int_0^\infty e^{-i\omega t}\,\langle \dot{A}(0)\,\dot{B}(t)\rangle\,dt. \tag{31}$$

Frequently, only the zero frequency ($\omega = 0$) value is of interest and then σ is simply the integral of the TCF. (Note the similarity to the average reorientation time, Eq. 27.) The generality of the fluctuation theory approach as expressed in Eq. 16 means that it can be straightforwardly extended to transport coefficients. Specifically, one obtains

$$E_{a,\sigma}(\omega) = -\frac{1}{\sigma(\omega)}\frac{\partial\sigma(\omega)}{\partial\beta} = \frac{\int_0^\infty e^{-i\omega t}\,\langle\delta H(0)\,\dot{A}(0)\,\dot{B}(t)\rangle\,dt}{\int_0^\infty e^{-i\omega t}\,\langle\dot{A}(0)\,\dot{B}(t)\rangle\,dt}, \quad (32)$$

for the frequency-dependent activation energy, which can be evaluated from simulations at a single temperature.

This expression is sufficiently general that it can be applied to properties including viscosity, conductivity, dielectric relaxation, and even spectroscopy. Indeed, Morita and co-workers have developed similar approaches to calculating the dependence of different vibrational spectra on temperature and other variables.[37–40] In the case of a number of the transport coefficients, *e.g.*, viscosity which is a focus on ongoing work in our group, the key difference with the diffusion and reorientational dynamics examples discussed above is that they involve quantities that are global. That is, the quantities A and B in the TCF depend on the full system configuration and are not obtained individually for each molecule. This means that the relevant TCF can require more averaging to converge, though this is in no way prohibitive.

5. Quantum Dynamics

The fluctuation theory for dynamics approach described above is completely general in that it can be applied to not only classical but also quantum mechanical, semiclassical, or mixed quantum-classical dynamics. Here we briefly consider the application to quantum dynamics. Consider a general quantum mechanical time correlation function,

$$C(t) = \langle\hat{A}(0)\,\hat{B}(t)\rangle = \frac{1}{\mathcal{Q}}\mathrm{Tr}[e^{-\beta\hat{H}}\,\hat{A}\,\hat{B}(t)], \quad (33)$$

where $\hat{B}(t) = e^{i\hat{H}t/\hbar}\hat{B}e^{-i\hat{H}t/\hbar}$, $\mathcal{Q}$ is the quantum mechanical partition function, and Tr is a quantum mechanical trace. Then, just as in the classical case, it is straightforward to show that the derivative with respect to β is given by

$$\frac{\partial C(t)}{\partial\beta} = \frac{1}{\mathcal{Q}}\mathrm{Tr}[e^{-\beta\hat{H}}\,\delta\hat{H}\,\hat{A}\,\hat{B}(t)], \quad (34)$$

where $\delta\hat{H} = \hat{H} - \langle\hat{H}\rangle$.

The thermal rate constant for a chemical reaction can be considered as a special example using the results of Miller, Schwartz, and Tromp.[10] They derived several equivalent forms for the formally exact quantum mechanical rate constant, including in terms of the flux-flux TCF,

$$k_{QM}(T) = \int_0^\infty C_{ff}(t)\,dt = \int_0^\infty \langle\hat{F}_s(0)\,\hat{F}_s(t)\rangle\,dt, \quad (35)$$

where $\hat{F}_s = i[\hat{H}, \theta(\hat{s} - s^\ddagger)]/\hbar$ is the symmetrized flux operator at the transition state dividing surface located at $s^\ddagger$. Then, using Eq. 34 the activation energy is given by

$$E_{a,QM} = \frac{\int_0^\infty \langle\delta\hat{H}(0)\,\hat{F}_s(0)\,\hat{F}_s(t)\rangle\,dt}{\int_0^\infty \langle\hat{F}_s(0)\,\hat{F}_s(t)\rangle\,dt}. \quad (36)$$

Note that $E_{a,QM}$ can be evaluated from the calculation of k_{QM} itself by one additional multiplication of the Hamiltonian. We have demonstrated the implementation (and accuracy) of this direct calculation of the activation energy for the simple one-dimensional Eckart barrier.[21] Similar activation energy expressions[21] can be obtained for each of the various TCFs that can be used to obtain the rate constant.[10]

III. BEYOND ACTIVATION ENERGIES

A. Non-Arrhenius Behavior

Thus far our discussion has focused on the temperature dependence of different dynamical quantities in the context of the activation energy. It is interesting to consider the situation where the activation energy is not sufficient to describe the the change in dynamics with temperature, *i.e.*, when it is itself temperature dependent. Indeed, a number of dynamical processes display strong non-Arrhenius behavior, *e.g.*, dynamics governed by low barriers in liquids or reaction rate constants that have a significant contribution from quantum mechanical tunneling. For example, liquid water displays significantly non-Arrhenius behavior in both reorientation dynamics[41,42] and diffusion,[19,20,43–46] from the deeply supercooled regime up to the boiling point.

The fluctuation theory for dynamics straightforwardly addresses non-Arrhenius behavior because it determines the analytical temperature derivatives completely locally at a single temperature, *e.g.*, at 298.15 K. In other words, it does not depend on any numerical derivative approximation such as that implicit in an Arrhenius analysis, which can be sensitive to the choice of temperatures. Moreover, the approach is not limited to the first derivative and higher derivatives can also be calculated. For example, for reorientational dynamics it can be shown that taking the derivative of Eq. 25 gives

$$\frac{\partial^2 C_2(t)}{\partial\beta^2} = \langle[\delta H(0)^2 - \langle\delta H^2\rangle]\,P_2\,[\vec{e}(t)\cdot\vec{e}(0)]\rangle \equiv C_{2,\delta H^2}(t), \quad (37)$$

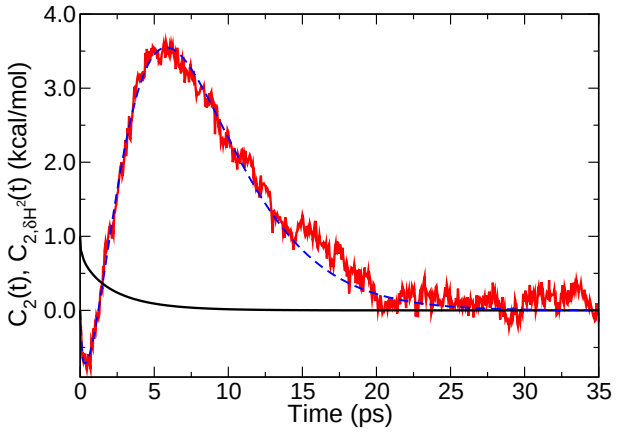

FIG. 6: The second-derivative reorientational TCF, $C_{2,\delta H^2}(t)$, is shown (red line) for SPC/E water at 298 K from 30,000 NVE trajectories along with a fit based on Eq. 26 (dashed blue line); $C_2(t)$ is shown for comparison (black line).

which is the first measure of non-Arrhenius behavior. This is analogous to an expression for the temperature derivative of the activation energy developed by Truhlar and Kohen in the context of non-Arrhenius enzyme kinetics.[47]

An example of this non-Arrhenius TCF is shown in Fig. 6, where $C_{2,\delta H^2}(t)$ is plotted as a function of time for OH reorientation in water at 298 K. These results were obtained using the same approach described in Ref. 48 with 30,000 short NVE trajectories. The expected behavior of $C_{2,\delta H^2}(t)$ is obtained by taking the second derivative with respect to β of the fitting function for $C_2(t)$ itself, Eq. 26. This fit is also presented in Fig. 6 and provides an excellent representation of the calculated TCF. The integral of $C_{2,\delta H^2}(t)$ is directly related to the non-Arrhenius behavior of the integrated reorientation time, Eq. 27, namely $\partial E_{a,\langle\tau_2\rangle}/\partial\beta$. The SPC/E model gives $\partial E_{a,\langle\tau_2\rangle}/\partial\beta = 4.81$ (kcal/mol)^2 at room temperature, compared to 7.66 (kcal/mol)^2 obtained by fitting the measured $\langle\tau_2\rangle$ values of Ludwig *et al.*[41] This is reasonable agreement, but the difference is indicative of the shortcomings of the SPC/E model in terms of describing the water reorientational dynamics over a broader range of temperatures.[33]

B. Activation Volumes

The fluctuation theory for dynamics can be extended to derivatives with respect to other thermodynamic variables.[27,49] For example, in the isothermal-isobaric ensemble the average of the dynamical quantity $f(t)$, given in Eq. 18, can be differentiated with respect to pressure to give

$$\frac{\partial\langle f(t)\rangle}{\partial p} = -\beta\,\langle\delta V(0) f(t)\rangle_{NpT} \tag{38}$$

where $\delta V(0) = V(0) - \langle V\rangle_{NpT}$. Such derivatives are related to the activation volume, which for a rate constant k is given by

$$\Delta V^{\ddagger} = -RT\frac{\partial \ln k}{\partial p}. \tag{39}$$

This measure of the pressure dependence of the rate constant is important in many practical situations of high-pressure chemistry but also interesting from a mechanistic viewpoint.[50,51] The typical interpretation of $\Delta V^{\ddagger}$ is as a measure of relative size of the transition state and reactant structures. However, Ladanyi and Hynes showed that this perspective is only complete in condensed phases if it includes the surrounding solvent molecules and their arrangement (or packing) around the transition state and reactants.[52]

The fluctuation theory for dynamics offers an improved method for calculating activation volumes from MD simulations. The typical approach involves calculation of k over a large pressure range (often spanning thousands of bar) to resolve the comparatively modest differences with pressure which are then used in an Arrhenius analysis to calculate a single activation volume.[51–54] This assumes that $\Delta V^{\ddagger}$ is p-independent, which is not true in some key cases, such as water diffusion. Alternatively, one can use simulations to estimate the volumes directly,[55] or calculate k at many pressures and fit the global pressure dependence which can then be used to determine $\Delta V^{\ddagger}$.

As an example of the fluctuation theory approach, consider the pressure dependence of the diffusion coefficient. From Eq. 38 it can be seen that the pressure derivative of the mean-squared displacement can be written as

$$\begin{aligned}\Delta V_D^{\ddagger} = -\frac{\partial \ln D}{\partial p} &= \frac{\lim\limits_{t\to\infty}\langle\delta V(0)\,|\vec{r}(t)-\vec{r}(0)|^2\rangle}{\lim\limits_{t\to\infty}\langle|\vec{r}(t)-\vec{r}(0)|^2\rangle} \\ &= \frac{\lim\limits_{t\to\infty} MSD_V(t)}{\lim\limits_{t\to\infty} MSD(t)},\end{aligned} \tag{40}$$

where $MSD_V(t) \equiv \langle\delta V(0)\,|\vec{r}(t)-\vec{r}(0)|^2\rangle_{NpT}$ in analogy to $MSD_H(t)$ obtained in deriving the activation energy. Indeed, this result is reminiscent of Eq. 24 and the interpretation is analogous. Namely, the activation volume is a measure of how the diffusion speeds up (or slows down) when the system volume is larger ($\Delta V > 0$) or smaller ($\Delta V < 0$) than its average value at the pressure of interest.

The diffusion coefficient of water is a key example of a property that does not exhibit an Arrhenius-like pressure dependence. As the pressure is increased, it is observed that D first increases ($\Delta V_D^{\ddagger} < 0$) and then decreases ($\Delta V_D^{\ddagger} > 0$).[17–20] The former behavior is attributed to

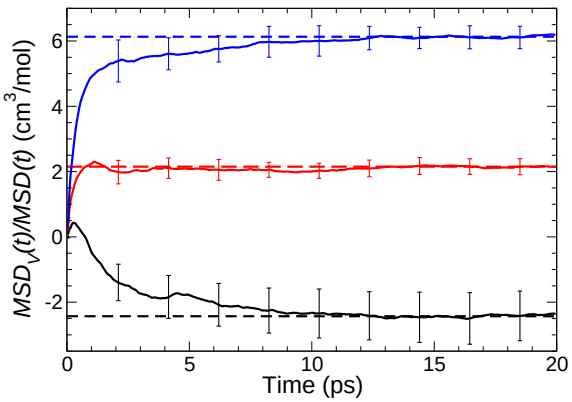

FIG. 7: The ratio $MSD_V(t)/MSD(t)$, which at long times is equal to the diffusion activation volume, $\Delta V_D^{\ddagger}$, for 100 bar and $T = 283$ (black), 383 (red), and 473 K (blue) for TIP4P/2005 water from 5,000 NVE trajectories. Dashed lines of the same color indicate the derived $\Delta V_D^{\ddagger}$ from fitting to $t \geq 15$ ps. Reprinted from Piskulich, Z. A., Mesele, O. O., and Thompson, W. H. *J. Chem. Phys.*, **2018**, *148*, 134105, with the permission of AIP Publishing.

disruption of the H-bonding network, while the latter is ascribed to significant distortion of the network at higher pressures such that the transition state for H-bond exchange requires a larger volume. For a fixed pressure, the activation volume increases with temperature, which is illustrated in Fig. 7, where the ratio $MSD_V(t)/MSD(t)$ and the corresponding $\Delta V_D^{\ddagger}$ values are plotted versus time at 100 bar for three temperatures. The activation volumes obtained are within $\sim$ 25% of the values obtained experimentally by Krynicki *et al.*[19]

IV. SUMMARY

Approaches for direct calculation of the activation energy for nearly any dynamical timescale of a chemical system from simulations at a single temperature have been presented. These methods directly calculate the analytical derivative with respect to temperature, in contrast to the standard Arrhenius analysis which determines the derivative numerically. They are fundamentally an application of fluctuation theory in statistical mechanics applied to dynamical properties.

The fluctuation theory approach enables new mechanistic insight. The activation energy can be rigorously decomposed into contributions associated with different terms in the Hamiltonian, *i.e.*, interactions present in the system. These are readily understood in the context of Tolman's interpretation of the activation energy as the difference between the average energy of reacting species relative to the average energy of the reactants.[5] Then each contribution is the average energy of a particular interaction (or kinetic energy) for the reacting species relative to that of the reactants. In other words, we can obtain the measure of how effective it is, in terms of accelerating the dynamics of interest, to deposit energy into specific interactions and motions of the molecular system.

The method is not limited to activation energies. Non-Arrhenius behavior can be probed by calculation of higher derivatives of a timescale with respect to temperature. Moreover, the change in dynamics with respect to nearly any thermodynamic variable can be determined by carrying out simulations in the appropriate ensemble.

A number of advantages associated with this approach have yet to be fully explored. A key example is that it permits access to activation energies even for systems that are at the point of a thermally-induced transformation, because simulations at only one temperature are required. Thus, an activation energy can be calculated for a liquid close to its boiling point or a protein near its melting temperature; for these systems an Arrhenius analysis is challenging because an increase in temperature generates a phase or structural change. In addition, we have only shown here some of the simplest possible decompositions of the activation energy into broad categories of interactions and the kinetic energy. Significantly more detailed mechanistic insight is available by considering the contributions to the energy of particular atomic or molecular interactions and motions.

ACKNOWLEDGMENTS

This work was supported by the National Science Foundation under Grant No. CHE-1800559. This material is based upon work supported by the National Science Foundation Graduate Research Fellowship under Grant Nos. 1540502 and 1451148 (Z.A.P.). The calculations were performed at the University of Kansas Center for Research Computing (CRC).

[1] A. Arrhenius, "Über die Reaktionsgeschwindigkeit bei der Inversion von Rohrzucker durch Saüren," Z. physik. Chem. **4**, 226–248 (1889).
[2] M. Menzinger and R. Wolfgang, "The Meaning and Use of the Arrhenius Activation Energy," Angew. Chem. Intl. Ed. **8**, 438–444 (1969).
[3] S. R. Logan, "The Origin and Status of the Arrhenius Equation," J. Chem. Educ. **59**, 279–281 (1982).
[4] K. J. Laidler, "The Development of the Arrhenius Equation," J. Chem. Educ. **61**, 494–5 (1984).
[5] R. C. Tolman, "Statistical Mechanics Applied to Chemical Kinetics," J. Am. Chem. Soc. **42**, 2506–2528 (1920).
[6] D. G. Truhlar, "Interpretation of the Activation Energy," J. Chem. Ed. **55**, 309–311 (1978).
[7] R. D. Levine and R. B. Bernstein, *Molecular Reaction Dynamics and Chemical Reactivity* (Oxford University Press, New York, 1987).
[8] N. C. Blais, D. G. Truhlar, and B. C. Garrett, "Dynamical Calculation of the Temperature Dependence of the Activation Energy

for a Chemical Reaction from 444 to 2400 K," J. Phys. Chem. **85**, 1094–1096 (1981).
[9]H. Rafatijo and D. L. Thompson, "General Application of Tolman's Concept of Activation Energy," J. Chem. Phys. **147**, 224111 (2017).
[10]W. H. Miller, S. D. Schwartz, and J. W. Tromp, "Quantum Mechanical Rate Constants for Bimolecular Reactions," J. Chem. Phys. **79**, 4889–4898 (1983).
[11]H. Eyring, "The Activated Complex in Chemical Reactions," J. Chem. Phys. **3**, 107–115 (1935).
[12]E. Wigner, "The Transition State Method," Trans. Faraday Soc. **34**, 29–41 (1938).
[13]T. L. Hill, *Statistical Mechanics. Principles and Selected Applications* (Dover, New York, 1956).
[14]L. D. Landau and E. M. Lifshitz, *Statistical Physics* (Addison-Wesley, Reading, MA, 1969).
[15]R. F. Greene and H. B. Callen, "On the Formalism of Thermodynamic Fluctuation Theory," Phys. Rev. **83**, 1231–1235 (1951).
[16]An analogous direct analysis of classical trajectories based on the Tolman expression for the activation energy, Eq. 3, has been previously applied[8] to the gas phase H + H_2 reaction to differentiate the contributions of relative translational motion and internal energy.
[17]L. A. Woolf, "Tracer Diffusion of Tritiated Water (THO) in Ordinary Water (H_2O) under Pressure," J. Chem. Soc., Faraday Trans. 1 **71**, 784–13 (1975).
[18]D. J. Wilbur, T. DeFries, and J. Jonas, "Self-Diffusion in Compressed Liquid Heavy-Water," J. Chem. Phys. **65**, 1783–1786 (1976).
[19]K. Krynicki, C. D. Green, and D. W. Sawyer, "Pressure and Temperature Dependence of Self-diffusion in Water," Faraday Discuss. Chem. Soc. **66**, 199–208 (1978).
[20]K. R. Harris and L. A. Woolf, "Pressure and Temperature Dependence of the Self Diffusion Coefficient of Water and Oxygen-18 Water," J. Chem. Soc., Faraday Trans. 1 **76**, 377–379 (1980).
[21]O. O. Mesele and W. H. Thompson, "Removing the Barrier to the Calculation of Activation Energies," J. Chem. Phys. **145**, 134107 (2016).
[22]D. Chandler, "Statistical Mechanics of Isomerization Dynamics in Liquids and the Transition State Approximation," J. Chem. Phys. **68**, 2959–2970 (1978).
[23]S. H. Northrup and J. T. Hynes, "The Stable States Picture of Chemical Reactions. I. Formulation for Rate Constants and Initial Condition Effects," J. Chem. Phys. **73**, 2700–2714 (1980).
[24]R. F. Grote and J. T. Hynes, "The Stable States Picture of Chemical Reactions. II. Rate Constants for Condensed Phase and Gas Phase Reaction Models," J. Chem. Phys. **73**, 2715–2732 (1980).
[25]C. Dellago and P. G. Bolhuis, "Activation Energies from Transition Path Sampling Simulations," Mol. Simul. **30**, 795–799 (2004).
[26]C. S. Lo, R. Radhakrishnan, and B. L. Trout, "Application of Transition Path Sampling Methods in Catalysis: A New Mechanism for CC Bond Formation in the Methanol Coupling Reaction in Chabazite," Catalysis Today **105**, 93–105 (2005).
[27]E. E. Borrero and C. Dellago, "Overcoming Barriers in Trajectory Space: Mechanism and Kinetics of Rare Events via Wang–Landau Enhanced Transition Path Sampling," J. Chem. Phys. **133**, 134112–12 (2010).
[28]C. Drechsel-Grau and M. Sprik, "Activation Energy for a Model Ferrous-Ferric Half Reaction from Transition Path Sampling," J. Chem. Phys. **136**, 034506–11 (2012).
[29]M. Moqadam, E. Riccardi, T. T. Trinh, A. Lervik, and T. S. van Erp, "Rare Event Simulations Reveal Subtle Key Steps in Aqueous Silicate Condensation," Phys. Chem. Chem. Phys. **19**, 13361–13371 (2017).
[30]M. Moqadam, A. Lervik, E. Riccardi, V. Venkatraman, B. Alsberg, and T. S. van Erp, "Local Initiation Conditions for Water Autoionization," Proc. Natl. Acad. Sci. **115**, E4569–E4576 (2018).
[31]P. G. Bolhuis and G. Csányi, "Nested Transition Path Sampling," Phys. Rev. Lett. **120**, 250601 (2018).
[32]H. J. C. Berendsen, J. R. Grigera, and T. P. Straatsma, "The Missing Term in Effective Pair Potentials," J. Phys. Chem. **91**, 6269–6271 (1987).
[33]J. L. F. Abascal and C. Vega, "A General Purpose Model for the Condensed Phases of Water: TIP4P/2005," J. Chem. Phys. **123**, 234505 (2005).
[34]R. G. Gordon, "Relations between Raman Spectroscopy and Nuclear Spin Relaxation," J. Chem. Phys. **42**, 3658–3665 (1965).
[35]Z. A. Piskulich and W. H. Thompson, "The Activation Energy for Water Reorientation Differs between IR Pump-probe and NMR Measurements," J. Chem. Phys. **149**, 164504 (2018).
[36]R. Zwanzig, "Time-Correlation Functions and Transport Coefficients in Statistical Mechanics," Annu. Rev. Phys. Chem. **16**, 67–102 (1965).
[37]S. Sakaguchi, T. Ishiyama, and A. Morita, "Theory and Efficient Computation of Differential Vibrational Spectra," J. Chem. Phys. **140**, 144109 (2014).
[38]S. Sakaguchi, T. Ishiyama, and A. Morita, "Theory and Efficient Computation of Differential Vibrational Spectra (vol 140, 144109, 2014)," J. Chem. Phys. **141** (2014).
[39]T. Joutsuka and A. Morita, "Improved Theory of Difference Vibrational Spectroscopy and Application to Water," J. Chem. Theor. Comp. **12**, 5026–5036 (2016).
[40]T. Joutsuka and A. Morita, "Efficient Computation of Difference Vibrational Spectra in Isothermal-Isobaric Ensemble," J. Phys. Chem. B **120**, 11229–11238 (2016).
[41]R. Ludwig, F. Weinhold, and T. C. Farrar, "Experimental and Theoretical Determination of the Temperature Dependence of Deuteron and Oxygen Quadrupole Coupling Constants of Liquid Water," J. Chem. Phys. **103**, 6941–6950 (1995).
[42]J. Qvist, C. Mattea, E. P. Sunde, and B. Halle, "Rotational Dynamics in Supercooled Water from Nuclear Spin Relaxation and Molecular Simulations," J. Chem. Phys. **136**, 204505 (2012).
[43]H. R. Pruppacher, "Self-Diffusion Coefficient of Supercooled Water," J. Chem. Phys. **56**, 101–107 (1972).
[44]K. T. Gillen, D. C. Douglass, and M. J. R. Hoch, "Self-Diffusion in Liquid Water to -31°C," J. Chem. Phys. **57**, 5117–5119 (1972).
[45]C. A. Angell, E. D. Finch, L. A. Woolf, and P. Bach, "Spin-Echo Diffusion Coefficients of Water to 2380 Bar and -20°C," J. Chem. Phys. **65**, 3063–3074 (1976).
[46]F. X. Prielmeier, E. W. Lang, R. J. Speedy, and H. D. L u demann, "The Pressure-Dependence of Self-Diffusion in Supercooled Light and Heavy-Water," Ber Bunsen Phys Chem **92**, 1111–1117 (1988).
[47]D. G. Truhlar and A. Kohen, "Convex Arrhenius Plots and their Interpretation," Proc. Natl. Acad. Sci. **98**, 848–851 (2001).
[48]Z. A. Piskulich, O. O. Mesele, and W. H. Thompson, "Removing the Barrier to the Calculation of Activation Energies: Diffusion Coefficients and Reorientation Times in Liquid Water," J. Chem. Phys. **147**, 134103–6 (2017).
[49]Z. A. Piskulich, O. O. Mesele, and W. H. Thompson, "Expanding the Calculation of Activation Volumes: Self-diffusion in Liquid Water," J. Chem. Phys. **148**, 134105 (2018).
[50]R. van Eldik, T. Asano, and W. J. le Noble, "Activation and Reaction Volumes in Solution. 2," Chem. Rev. **89**, 549–688 (1989).
[51]A. Drljaca, C. D. Hubbard, R. van Eldik, T. Asano, M. V. Basilevsky, and W. J. le Noble, "Activation and Reaction Volumes in Solution. 3," Chem. Rev. **98**, 2167–2290 (1998).
[52]B. M. Ladanyi and J. T. Hynes, "Transition-State Solvent Effects on Atom Transfer Rates in Solution," J. Am. Chem. Soc. **108**, 585–593 (1986).
[53]S. Kerisit and K. M. Rosso, "Transition Path Sampling of Water Exchange Rates and Mechanisms around Aqueous Ions," J. Chem. Phys. **131**, 114512–15 (2009).
[54]L. X. Dang and G. K. Schenter, "Solvent Exchange in Liquid Methanol and Rate Theory," Chem. Phys. Lett. **643**, 142–148 (2016).

[55]H. Wiebe, J. Spooner, N. Boon, E. Deglint, E. Edwards, P. Dance, and N. Weinberg, "Calculation of Molecular Volumes and Volumes of Activation Using Molecular Dynamics Simulations," J. Phys. Chem. C **116**, 2240–2245 (2012).

TOC Graphic